Geomechanics and Engineering, *Vol. 34, No. 2 (2023) 197-208*
https://doi.org/10.12989/gae.2023.34.2.197

Rate-dependent shearing response of Toyoura sand addressing influence of initial density and confinement: A visco-plastic constitutive approach

Mousumi Mukherjee* and Siddharth Pathak[a]

School of Civil and Environmental Engineering, Indian Institute of Technology Mandi, Mandi-175075, H.P., India

(*Received February 20, 2022, Revised May 19, 2023, Accepted June 15, 2023*)

Abstract. Rate-dependent mechanical response of sand, subjected to loading of medium to high strain rate range, is of interest for several civilian and military applications. Such rate-dependent response can vary significantly based on the initial density state of the sand, applied confining pressure, considered strain rate range, drainage condition and sand morphology. A numerical study has been carried out employing a recently proposed visco-plastic constitutive model to explore the rate-dependent mechanical behaviour of Toyoura sand under drained triaxial loading condition. The model parameters have been calibrated using the experimental data on Toyoura sand available in published literature. Under strain rates higher than a reference strain rate, the simulation results are found to be in good agreement with the experimentally observed characteristic shearing behaviour of sand, which includes increased shear strength, pronounced post-peak softening and suppressed compression. The rate-dependent response, subjected to intermediate strain rate range, has further been assessed in terms of enhancement of peak shear strength and peak friction angle over varying initial density and confining pressure. The simulation results indicate that the rate-induced strength increase is highest for the dense state and such strength enhancements remain nearly independent of the applied confinement level.

Keywords: drained triaxial shearing; numerical modelling; rate-dependent response; strain rate effect; Toyoura sand; visco-plastic constitutive model

1. Introduction

Mechanical behavior of sand under medium to high strain rate loading has been of interest for several geotechnical applications such as explosions and air blasts, mine blasts, projectile penetration, dynamic compaction, installation of deep-sea anchors, pile driving and rapid load testing of piles etc. The mechanical response of sand has also been noticed to vary markedly in laboratory transient tests with strain rate ranging between 10^{-5} /s to 1 /s or even higher (Casagrande and Shannon 1949, Whitman 1957, Whitman and Healy 1962, Lee *et al.* 1969, Jackson *et al.* 1980, Farr 1986, 1990, Yamamuro and Lade 1993, Abrantes and Yamamuro 2002, Yamamuro *et al.* 2011, Watanabe and Kusakabe 2013, Suescun-Florez and Iskander 2017). Rate effect in sand is generally manifested by an apparent enhancement of soil strength and stiffness, and noticed to vary significantly with the change in level of confinement, density state, moisture content, drainage condition, particle shape, size, gradation and mineralogy (Omidvar *et al.* 2012, Suescun-Florez *et al.* 2015). Such variation is generally attributed to the change in the underlying mechanisms of rate-induced strength mobilization, which includes suppressed particle rearrangement under loading with medium to high strain rate and subsequent volume change tendencies, inertial and viscous effect, and reduced particle crushing associated with higher rates (Whitman and Healy 1962, Karimpour and Lade 2010, Yamamuro *et al.* 2011, Omidvar *et al.* 2012, Prabhu and Qiu 2022). The rate-dependent response is generally assessed in terms of peak shear strength, post-peak stress response, peak friction angle, volumetric or pore pressure response over the applied strain range and strain at peak shear stress.

The density and confinement state plays an important role on the observed rate-induced response of sand. The rate effects in dense sand are noticed to be more pronounced than in loose sand (Lee *et al.* 1969, Yamamuro *et al.* 2011, Suescun-Florez and Iskander 2017). Moreover, in case of loose sand, such effects become evident at low confinement due to suppressed compression arising from restrained particle rearrangement along with the inertial and viscous effects (Whitman and Healy 1962). On the contrary, the rate effect in dense sand enhances markedly at high confinement due to influence of strain rate on the associated particle crushing phenomena (Karimpour and Lade 2010, Lade and Karimpour 2010, Suescun-Florez and Iskander 2017). The condition of increasing strain rate along with high confinement restricts the compressibility and hence, requiring more energy to attain the same level of strain in order to initiate particle crushing that further results in increased strength. Degree of saturation and drainage condition has also been noticed to influence the rate-induced strength enhancement of sand. For example, strain rate effect has been reported to be more pronounced in the saturated sand as compared to the dry one, where primarily

*Corresponding author, Assistant Professor
E-mail: mousumi@iitmandi.ac.in
[a]Ph.D. Student
E-mail: d18019@students.iitmandi.ac.in

ISSN: 2005-307X (Print), 2092-6219 (Online)

suppressed particle rearrangement results in an increase in the peak friction angle and initial shear modulus (Whitman, 1957, Watanabe and Kusakabe 2013). For drained shearing of saturated sand, high strain rates often lead to partial drainage condition and subsequent generation of residual pore water pressure can significantly alter the rate-dependent response of sand (Seed and Lundgren 1954). For saturated case, the shear strength increment with increasing strain rate is attributed to a combined mechanism of viscous effect and consolidation process involving dissipation of excess pore water pressure. It is to be noted that the suppressed volumetric response of sand at high strain rate translates to a noticeable change in the pore water pressure response when subjected to undrained condition. This further leads to more prominent rate effect phenomena in sands subjected to undrained tests in comparison to the drained one (Seed and Lundgren 1954, Yamamuro and Lade 1993, Watanabe and Kusakabe 2013).

The shape, size and gradation of particles also influence the rate-dependent response of sand considerably (Kongkitkul *et al.* 2008). In comparison to the rounded or subrounded particles, angular particles provide higher interlocking and hence, exerts more resistance to particle rearrangement under high strain rate (Omidvar *et al.* 2012). Studies also indicate that at high confinement, angular soils are more prone to grain crushing due to presence of more asperities resulting in local stress concentration (Emerson and Hendron 1971, Wang and Wong 2010). As a result, angular sands in general exhibit more pronounced rate effect phenomena compared to rounded and subrounded grains irrespective of the level of confinement (Mukherjee 2016). Similar to angularity, gradation also plays an important role on rate effect, e.g., well graded sand exhibits high interlocking resulting in enhanced resistance to particle rearrangement with increase in the strain rate (Whitman, 1957, Monkul 2013). Further, soils with finer particle sizes are more rate-sensitive due to lower permeability and subsequent development of larger pore water pressure variations when subjected to undrained condition with varying strain rate (Casagrande and Shannon 1949, Augustesen *et al.* 2004, Karunawardena *et al.* 2011, Safa *et al.* 2019, Chen *et al.* 2019).

The implications of strain rate effect become imperative for rapid load testing of piles or pile jacking/driving process in medium to fine sands. Such field tests may result in an overestimated static bearing capacity owing to the increased shear strength at the applied loading rate (Holscher *et al.* 2012, Watanabe and Kusakabe 2013). However, there are very limited laboratory test data available on sand for the intermediate range of strain rate (10^{-5} /s to 1 /s), which is pertinent to such field problems (Suescun-Florez and Iskander 2017). Furthermore, majority of such tests were primarily focused on rate effects associated with crushing phenomena and hence, reported experiments were conducted on either calcareous sands (Abrantes and Yamamuro 2002, Yamamuro *et al.* 2011) or silica sand with high level of confinement (Lee *et al.* 1969, Yamamuro and Lade 1993). The rate-induced strength enhancement in sand over varying density and confining pressure range needs to be explored in further details and in this regard, use of a robust constitutive model in conjunction with available test data can be very effective. Following the mathematical framework of Perzyna (1963, 1966), overstress type visco-plastic models have often been employed in the past to mimic the rate-dependent behaviour of sand (Katona 1984, Desai and Zhang 1987, Boukpeti *et al.* 2004, Tong and Tuan 2007, Martindale *et al.* 2010, Andrade *et al.* 2012, Higgins *et al.* 2013, Shi *et al.* 2021). Most of these models are based on the critical state concept, governed by volumetric strain hardening, and predicts evolution of viscoplastic strain rate based on Perzyna type modified flow rule. Recently, Mukherjee *et al.* (2021) has proposed a non-associative overstress type visco-plastic model with both shear and volumetric hardening. The proposed model can aptly capture some of the key features of the rate-dependent strength characteristics of sand, namely the distinct peaks with enhanced shear strength, pronounced post-peak softening and suppressed compression. With a proper calibration of the constitutive parameters, the proposed model exhibits potential to predict rate-dependent response of sand over different density states and confining pressure ranges.

In the present study, the visco-plastic model of Mukherjee *et al.* (2021) has been employed for the assessment of rate-dependent mechanical behaviour of Toyoura sand in reference to the drained triaxial experimental data available in the literature. The constitutive parameters are first calibrated based on the experiments reported over a range of strain rate and the model predictions are then validated against the drained triaxial experiments on dense Toyoura sand. The rate-dependent response of Toyoura sand, subjected to intermediate strain rate range, has further been assessed over varying initial density and confining pressure level in terms of enhancement of peak shear strength, peak friction angle, post-peak shear response and axial strain at peak.

2. Adopted visco-plastic constitutive model for capturing rate-dependent response

The recently proposed non-associative visco-plastic model by Mukherjee *et al.* (2021) has been employed here to mimic the rate-dependent response of Toyoura sand. The referred visco-plastic model extended the inviscid critical state based model of Wood *et al.* (1994) to a rate-dependent form employing Perzyna-type overstress formulation (Perzyna 1963). The visco-plastic model includes both shear and volumetric type hardening law. This dual hardening feature enables the model to capture the key observations related to the rate-dependent strength characteristics of sand, i.e., early peak with enhanced shear strength and suppressed compression. Such prediction capabilities of the employed model have been already examined by Mukherjee *et al.* (2021) while assessing the strain-rate dependent shearing behavior of silica and crushed coral sand based on the triaxial test data reported in Suescun-Florez and Iskander (2017) and Yamamuro *et al.* (2011), respectively.

The incremental constitutive relation as formulated

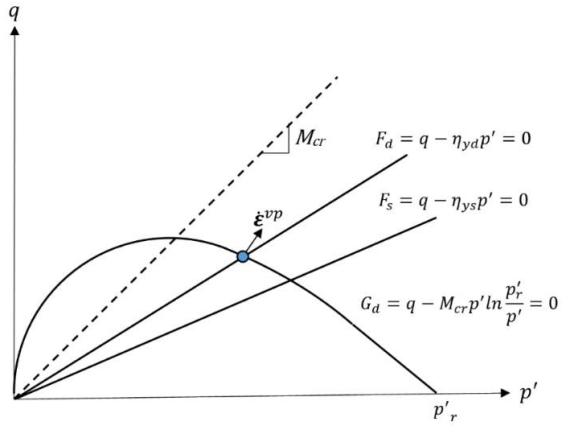

Fig. 1 Static and dynamic yield surface, plastic potential in the stress space

within a small deformation framework is given below

$$\dot{\sigma}'_{ij} = C_{ijkl}\left(\dot{\varepsilon}_{kl} - \dot{\varepsilon}^{vp}_{kl}\right) \tag{1}$$

where, σ'_{ij}, ε_{kl}, ε^{vp}_{kl} and C_{ijkl} represents the effective stress, total strain, visco-plastic strain and elastic stiffness tensor, respectively. The evolution of visco-plastic strain is governed by the Perzyna-type overstress formulation with two yield surfaces i.e., the dynamic (F_d) and static (F_s) yield surface, and a plastic potential (Fig. 1) as defined by the following

$$F_d = q - \eta_{yd}p' = 0 \tag{2}$$

$$F_s = q - \eta_{ys}p' = 0 \tag{3}$$

$$G_d = q - M_{cr}p'ln\frac{p'_r}{p'} = 0 \tag{4}$$

where, $p' = \sigma'_{ij}/3$ is the mean effective stress, $q = \sqrt{\frac{3}{2}S_{ij}S_{ij}}$ is the distortional shear stress or deviatoric stress, S_{ij} is the deviatoric stress tensor, η_{yd} and η_{ys} represent the dynamic and static shear stress ratios, M_{cr} is the shear stress ratio at critical state and p'_r is an arbitrary variable representing value of plastic potential function on the mean effective stress axis, respectively. The evolution of visco-plastic strain rate is governed by the following flow rule

$$\dot{\varepsilon}^{vp}_{ij} = \dot{\varepsilon}_{ref}\left(\frac{\eta_{yd}}{\eta_{ys}}\right)^n \frac{\partial G_d}{\partial \sigma'_{ij}}, \text{ when } \frac{\eta_{yd}}{\eta_{ys}} \geq 1 \tag{5}$$

where, $\dot{\varepsilon}_{ref}$ is the reference axial strain rate and n is the power law exponent controlling the rate-dependent behavior. The evolution of static shear stress ratio depends on the accumulated visco-plastic shear strain and follows a hyperbolic hardening relationship (Wood *et al.* 1994, Wood 2004) as given by the following

$$\frac{\eta_{ys}}{\eta_{ps}} = \frac{\varepsilon^{vp}_q}{a + \varepsilon^{vp}_q} \tag{6}$$

where, a is a model parameter which represents the visco-plastic shear strain required to reach a stress ratio of 50% of the static peak shear stress ratio η_{ps}, the expression for which is given as

$$\begin{aligned}\eta_{ps} &= M_{cr} - k\Psi = M_{cr} - k(v - \Gamma + \Lambda ln p') \\ &= M_{cr} - k[v_0(1 - \varepsilon_p) - \Gamma + \Lambda ln p']\end{aligned} \tag{7}$$

where, Ψ is a state variable representing the density state of soil with respect to the critical state at a particular mean stress, k is a model parameter linking state variable and peak shear strength ratio, Γ is the specific volume corresponding to mean effective stress of 1 kPa, Λ is the slope of critical state line in the compression plane, v_0 and v are the initial and current specific volume, respectively.

3. Calibration of constitutive parameters from drained triaxial test

A MATLAB code has been developed to simulate the strain controlled drained triaxial test condition following the newly proposed visco-plastic model. A fully explicit stress update algorithm has been employed for this purpose (Wang *et al.* 1997) and the same code has also been used for calibrating the constitutive model parameters. Considering the explicit nature of the time integration scheme, very small strain increments are chosen to avoid any numerical instability. The total number of iterations are so chosen that the accumulated total axial strain is 20%, which has been considered as the failure strain.

3.1 Calibration of model parameters pertinent to rate-independent response

In the present study, the constitutive model parameters pertinent to the rate-independent shearing response of Toyoura sand have been calibrated based on the drained triaxial test data at initial confining pressure $p'_0 = 100$ kPa and for three different initial void ratios (e_0) i.e., 0.67, 0.83 and 0.92 as reported in the available literature (Verdugo and Ishihara 1996, Watanabe and Kusakabe 2012). Toyoura sand, a Japanese benchmark sand, is usually characterized as an angular to sub-angular, fine grained, poorly graded sand and identified as SP by the Unified Soil Classification System (Safdar *et al.* 2021). The model parameters associated with the rate-independent shearing response are G_0, υ, a, k, M_{cr}, Γ and Λ. The shear and volumetric hardening related parameters, a and k, the critical state parameters M_{cr}, Γ and Λ, and the elastic parameter υ are independent of the initial confining pressure p'_0 and initial void ratio e_0. Whereas, the effect of initial confining pressure p'_0 and initial void ratio e_0 has been incorporated in the calculation of shear modulus G as illustrated in the following section.

The elastic response has been assumed to be a linear one and to start with, the Poisson's ratio υ has been calculated at an axial strain level of 1% from the volumetric and axial strain responses. Further, calculation of elastic shear modulus G has been carried out by scaling the small-strain shear modulus G_0 through a scaling factor, where G_0 depends on the initial specific volume v_0 and initial mean

effective stress p_0' (expressed in kPa) as given below (Hardin and Black 1966)

$$G_0 = 3230 \times \frac{(3.97 - v_0)^2}{v_0} \times \sqrt{p_0'} \quad (8)$$

In this study, a scaling factor of 12 has been noticed to best fit the experimental data of Toyoura sand. In addition, at a given initial confinement, an average G value has been adopted accounting for all the three different initial void ratio values. Next, the calibration of critical state parameters M_{cr}, Λ and Γ have been carried out. The critical state stress ratio M_{cr} has been estimated from stress ratios at 20% strain level and the calculations of Λ and Γ have been performed based on the critical state line plotted in the *e-ln p'* plane using the same strain level data. The model parameter a has been calibrated based on the normalized stress ratio vs shear strain plots corresponding to different initial void ratios at p_0'= 100 kPa and finally an average value of 0.0001 has been adopted. It is to be noted that the estimated values of a ranged between 0.0001-0.0008 with lower values corresponding to the higher void ratios or loose sand. As calibration has been conducted based on the experimental data reported from a single confining pressure, which is also relatively low in magnitude, i.e., p_0'= 100 kPa, the lower estimate of a value has been selected for the calibration purpose. The model parameter k connects the state variable Ψ to the peak shear strength ratio η_{ps} as illustrated in Eq. (7). It is to be noted that the parameter k does not have any direct physical significance. In order to calibrate k, first the critical state parameters, M_{cr}, Γ and Λ should be calibrated. With a calibrated probable range of these parameters from the experimental data, k can be further calibrated iteratively. This can make the calibration process very tedious. Moreover, the effect of k has been noticed to be less significant on the overall stress-strain and volumetric response of the soil when compared to the other parameters like M_{cr}, Γ and Λ (Wood *et al*. 1994). Hence, for the ease of the model parameter calibration process, the value of k has been adopted from the range of 1-2 as reported in Wood and Belkheir (1994) and Gajo and Wood (1999). The final calibrated values of the model parameters pertaining to the rate-independent analysis are reported in Table 1. Based on the estimated critical state parameter values, the critical state void ratio (e_c) has been estimated as 0.885 at the initial confining pressure of 100 kPa and, thereby, the considered void ratios, i.e., 0.67, 0.83 and 0.92, can be identified as dense, medium dense and loose initial states, respectively.

The simulated rate-independent drained triaxial responses of Toyoura sand, as obtained based on these calibrated parameters, have been plotted in Fig. 2 along with the experimental observations reported in literature (Verdugo and Ishihara 1996, Watanabe and Kusakabe 2012).

Table 1 Calibrated model parameters for Toyoura sand pertaining to rate-independent analysis

Parameter	υ	G (kPa)	M_{cr}	Λ	Γ	a	k
Value	0.3	$G_0/12$	1.15	0.025	2.0	0.0001	2

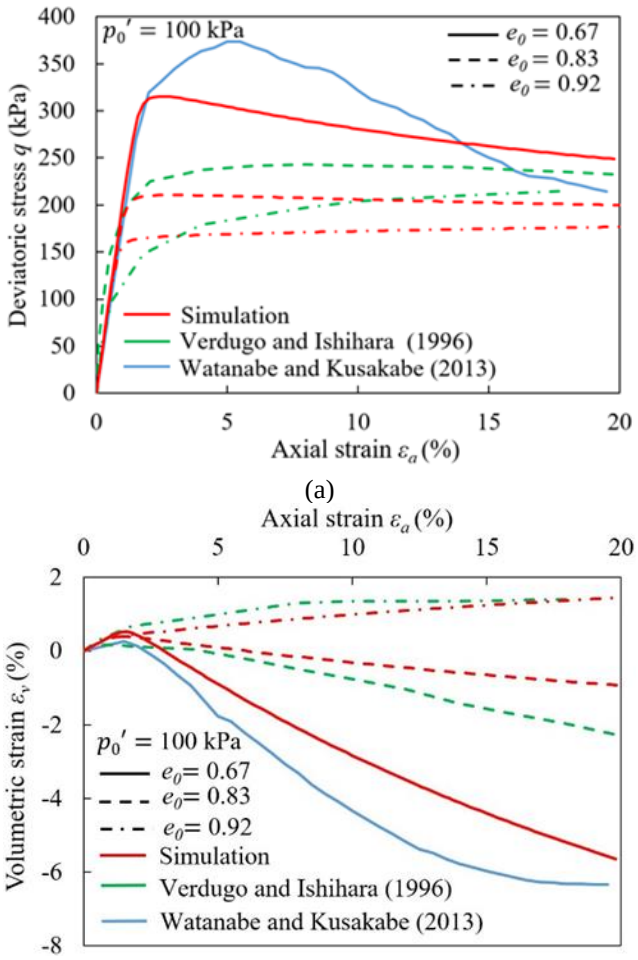

Fig. 2 Evolution of (a) stress-strain and (b) volumetric response of Toyoura sand subjected to rate-independent drained triaxial condition at 100 kPa initial confining pressure for three different initial densities (e_0 = 0.67, 0.83, 0.92)

It can be noticed that the employed model with the calibrated parameters can aptly capture the generic trend of the rate-independent stress-strain and volumetric response of Toyoura sand. This includes strength increment with increase in the density level along with a hardening response for loose sand, while a distinct peak followed by softening response for dense sand during the continued shearing. The simulated shear stress response has been noticed to underpredict the peak strength magnitudes for all three density states. Such underpredictions of the peak strength values are in the range of 10-15% for all these three densities. This kind of underprediction for the shear strength values will lead to a conservative design for the geotechnical application purposes, e.g., estimation of bearing capacity. Further, following the conventional calibration procedure, a manual iterative process has been adopted here for calibrating the constitutive model parameters. However, use of an optimization based algorithm or Bayesian update scheme for the parameter calibration process may improve the constitutive model

prediction through selection of an optimal set of parameter values. In case of volumetric response, compressive behavior has been noticed for the loose sand; whereas dilative behavior has been predicted during the shearing of dense sand. Further, the model can also predict the gradual change in the volumetric response of medium dense sand from a compressive to dilative one. The predicted volumetric responses, as well, are in close agreement with the experimental observation.

3.2 Calibration of model parameters pertinent to rate-dependent response

Watanabe and Kusakabe (2012) reported drained triaxial experiments on saturated dense Toyoura sand ($e_0 = 0.67$) at varying strain rate ranging from 5x10^{-5} /s to 2.5 /s. The same has been used for calibration of constitutive model parameters pertinent to the rate-dependent response. It was reported in Watanabe and Kusakabe (2012) that while performing the drained triaxial tests at $p_0' = 100$ kPa with strain rates 5x10^{-2} /s to 2.5 /s, a partial drainage condition was noticed. Such partial drainage led to development of negative pore water pressure, which further resulted into considerably higher shear stress development. Hence, only test data of strain rate range 5x10^{-5} /s to 5x10^{-1} /s has been selected for calibration and further validation study here. It is interesting to note that Seed and Lundgren (1954) also reported similar observation of partial drainage condition and associated strength increase in drained triaxial tests with high strain rate. Apart from saturated sand, triaxial test data on dry dense Toyoura sand, for the case with $p_0' = 100$ kPa, was also reported in Watanabe and Kusakabe (2012). The rate-induced strength enhancement was noticed to be higher for the saturated case in comparison to the dry one, especially at the relatively higher strain rate values (5x10^{-2} /s and 5x10^{-1} /s) where small amount of negative pore water pressure development was yet recorded. In the present study, both the saturated and dry cases have been considered for comparing the rate-induced strength enhancements in terms of the calibrated model parameters and their subsequent influence has been explored on the predicted strength behavior.

The lowest axial strain rate, i.e., 10^{-5} /s reported in the triaxial experiments of Watanabe and Kusakabe (2012), has been considered as the reference axial strain rate ($\dot{\varepsilon}_{ref}$) for the rate-dependent analysis. It is to be noted that a strain rate range in the order of 10^{-5} /s had often been employed in the past for performing quasi-static laboratory experiments, e.g. monotonic triaxial or biaxial tests on Toyoura sand (Park and Tatsuoka 1994, Li *et al.* 2009) or other sand types (Mokni and Desrues 1998, Doanh and Ibraim 2000, Azeiteiro *et al*. 2017), to explore the rate-independent shearing behavior. It supports the consideration of a similar strain rate range as threshold magnitude for $\dot{\varepsilon}_{ref}$. Further, the power law exponent n has been estimated from the peak deviatoric shear stress (q_p) based on the following expression

$$n = \log_{10}\frac{\dot{\varepsilon}}{\dot{\varepsilon}_{ref}} \Big/ \log_{10}\frac{q_p}{q_{p_{ref}}} \qquad (9)$$

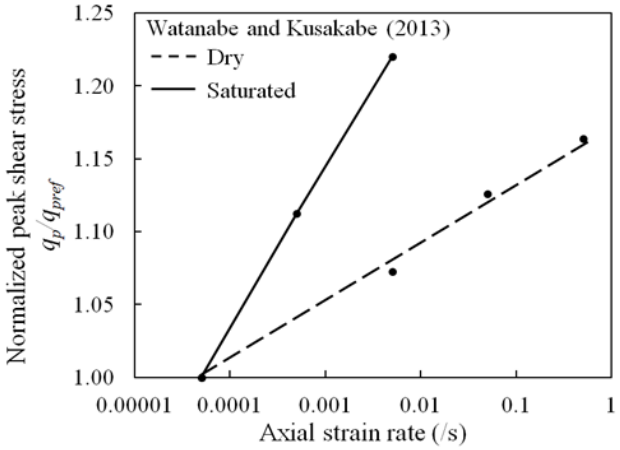

Fig. 3 Variation in the normalized peak shear stress ($q_p/q_{p_{ref}}$) of dense Toyoura sand ($e_0 = 0.67$) subjected to drained triaxial loading with a range of axial strain rate ($\dot{\varepsilon}$) and at an initial confining pressure (p_0') of 100 kPa

From the above relation, it can be observed that n value depends on the normalized peak shear stress ($q_p/q_{p_{ref}}$), current axial strain rate ($\dot{\varepsilon}$) and $\dot{\varepsilon}_{ref}$. The normalized peak shear stresses for both saturated and dry dense Toyoura sand over the considered strain rate range have been depicted in Fig. 3. The variation in the slopes of the trend lines for these two cases clearly reflects different level of rate-sensitivity. Accordingly, n value has been calculated for these two cases: for the dry case, it has been estimated to be approximately 45; whereas, n=25 has been identified for the saturated case. It can be observed from Eq. (9) that a lower value of n denotes higher rate-sensitivity reflecting higher peak shear strength at any given axial strain rate in comparison to the reference rate.

Subsequently, the rate-dependent drained triaxial simulations have been carried out at five different strain rates varying from 5x10^{-5} /s to 5x10^{-1}/s following the visco-plastic model of Mukherjee *et al.* (2021). In addition, rate-independent drained triaxial simulations have also been performed using the underlying inviscid model of Wood *et al.* (1994). The simulation results are compared against the experimental observations of Watanabe and Kusakabe (2012) on dense Toyoura sand as illustrated in Fig. 4. It can be noticed that the employed visco-plastic model with the calibrated parameters can predict the characteristic observations related to the stress-strain behavior of dense Toyoura sand at intermediate strain rate range. This includes a generic trend of strength increase and a delayed peak with pronounced post-peak softening. It is to be noted that the simulated stress-strain response with the rate-independent model coincides with the rate-dependent response at the

Hence, the experimental peak and post-peak responses are markedly higher in comparison to the shear responses at lower rates and the model also underpredicts the same. The volumetric response for the saturated drained test has been plotted in Fig. 4(c) and it indicates that the model predictions are of the same range as reported in the

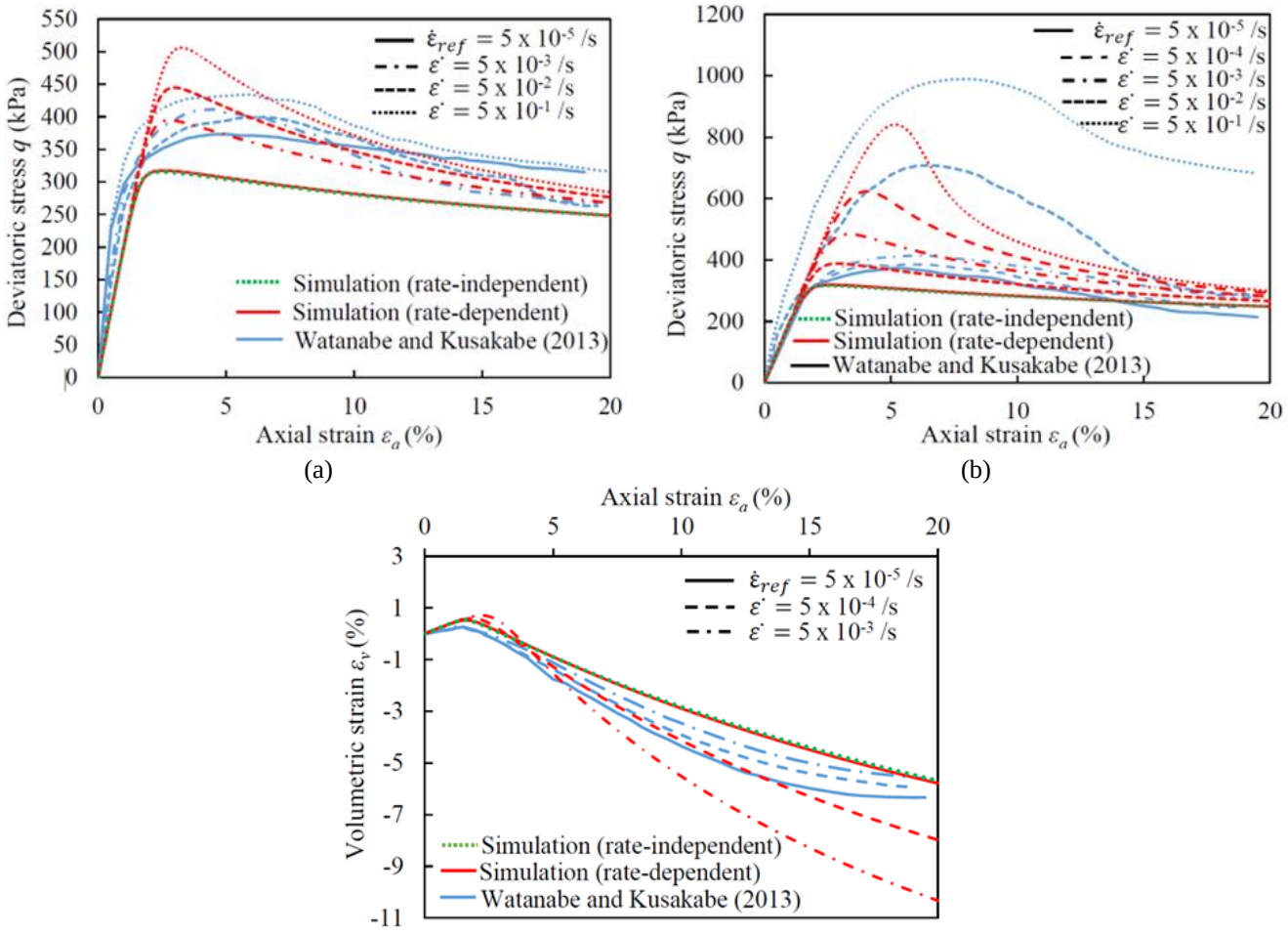

Fig. 4 Stress-strain response of (a) dry (n = 45) and (b) saturated (n = 25) dense Toyoura sand ($e_0 = 0.67$), and (c) volumetric response of saturated (n = 25) dense Toyoura sand ($e_0 = 0.67$) subjected to drained triaxial loading condition with initial confining pressure (p_0') of 100 kPa and varying strain rate

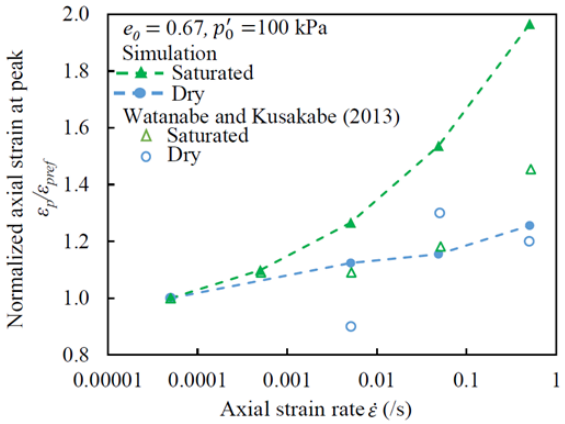

Fig. 5 Variation in the normalized axial strain at peak ($\varepsilon_p/\varepsilon_{p_{ref}}$) for dense Toyoura sand ($e_0 = 0.67$) over the selected strain rate range when subjected to drained triaxial condition with initial confining pressure (p_0') of 100 kPa

experiments. However, the model predicts an enhanced dilation trend with increasing strain rates instead of a suppressed dilation as observed in the experiments. The axial strains at peak for different strain rates have further been extracted and normalized with respect to the same at reference strain rate. The variation in the normalized axial strain at peak has been plotted in Fig. 5 along with the reported experimental values. The model rightly envisions a generic increasing trend for the axial strain at peak with increasing strain rate, which indicates a delayed onset of peak shear strength for the dense sand.

3.3 Validation for the predicted rate-dependent behavior employing visco-plastic model

Along with 100 kPa, drained triaxial shearing simulations have also been conducted at 500 kPa confining pressure with varying strain rate and the peak shear strength (q_p) magnitudes obtained from these simulations have been compared against the reported experimental values in Fig. 6(a). It is to be noted that the drained triaxial simulations at 500 kPa confinement have been conducted with n = 45 as no information over generation of excessive pore water pressure has been reported in Watanabe and Kusakabe (2012) at this higher confinement under increased strain rate. Further, the overall stress-strain and volumetric

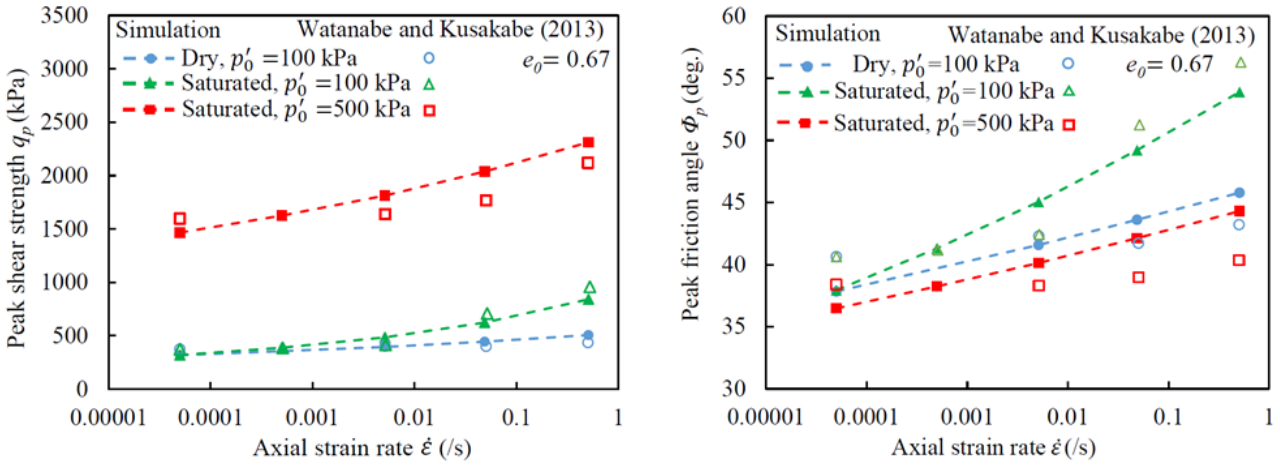

Fig. 6 Variation in the (a) peak shear strength (q_p) and (b) peak friction angle (Φ_p) of dense Toyoura sand ($e_0 = 0.67$) subjected to drained triaxial condition at two different initial confinement ($p_0' = 100$, 500 kPa) and varying strain rate

responses at different strain rate have also not been reported at this confinement; however, the experimental triaxial data of peak shear stress and peak friction angle have been reported for this confinement at various strain rates. Hence, while carrying out the validation study with the calibrated model parameters, comparison has been made between the reported experimental values of these strength parameters at 500 kPa confinement against the obtained numerical results from the visco-plastic constitutive model. It can be observed that in similitude to the predictions of 100 kPa confinement with different saturation condition, the estimated peak shear strength magnitudes at 500 kPa are comparable with the experimental data and indicates significant strength enhancement with increasing strain rate. Further, the peak friction angle (Φ_p) values have also been estimated from the peak shear strength observations and presented in Fig. 6(b). For the saturated drained case at lower confinement, the rate-induced strength increase is around 160% as compared to the case at higher confinement or for the dry one at lower confinement, where such enhancement is in the range of 60%. Interestingly, the corresponding increase in the peak friction angles are in the range of 40% and 20%, respectively.

4. Rate-dependent behavior of Toyoura sand over different initial void ratio and confining pressure range

The visco-plastic constitutive model in conjunction with the calibrated model parameters has further been used to explore the rate-dependent response of Toyoura sand over different density and confining pressure range. In this regard, two different initial confining pressures, i.e., p_0' =100 kPa and 500 kPa, have been considered along with three density states with initial void ratios as $e_0 = 0.92$, 0.83 and 0.67, which represents loose, medium dense and dense states, respectively. The stress-strain and volumetric responses for dense sand subjected to p_0' =100 kPa have already been discussed in the previous section. The simulation results for medium dense ($e_0 = 0.83$) and loose ($e_0 = 0.92$) sand at p_0' =100 have further been plotted in Fig. 7. It can be noticed from Figs. 7(a) and 7(b) that medium dense sand exhibits a similar behavior as that of dense sand with enhanced shear strength having a distinct peak followed by post- peak softening at the higher strain rates. In case of volumetric response, an enhanced dilation or reduced compression has been observed with increase in the strain rate. For loose sand, a hardening type stress-strain response has been predicted by the model at low strain rate with volumetric compression (Figs. 7(a) and 7(b)). However, with increase in strain rate, a phase transformation can be noticed with volumetric response changing from compressive to a dilative one (Fig. 7(d)). This observation is consistent with the existing rate-effect related experimental literature available for other sands (Omidvar *et al.* 2012) and such enhanced dilation at increasing rate is indicative of tendency of suppressed particle rearrangement. The increased volumetric dilation term further results a decrease in the peak stress ratio η_{ps} (Eq. (7)), which governs the softening response during shearing at higher rate as depicted in Fig. 7(c). In case of loose soil, such rate-induced softening at higher rate was also noticed experimentally by earlier researchers (Yamamuro *et al.* 2011, Suescun-Florez and Iskander, 2017). In the following sections, the rate-induced strength enhancements are further assessed in form of increment in peak shear strength, peak friction angle and variation in the axial strain at peak for the selected density and pressure range.

4.1 Peak shear strength

The variation of peak shear strengths (q_p) over the strain rate ranges has been presented in Fig. 8(a) along with a normalized peak shear strength plot in Fig. 8(b). The peak shear strength variation can be noticed to be maximum for dense Toyoura sand ($e_0 = 0.67$) with an enhancement of nearly 60% for four orders of magnitude increase in the logarithmic scale of strain rate. However, such increase is

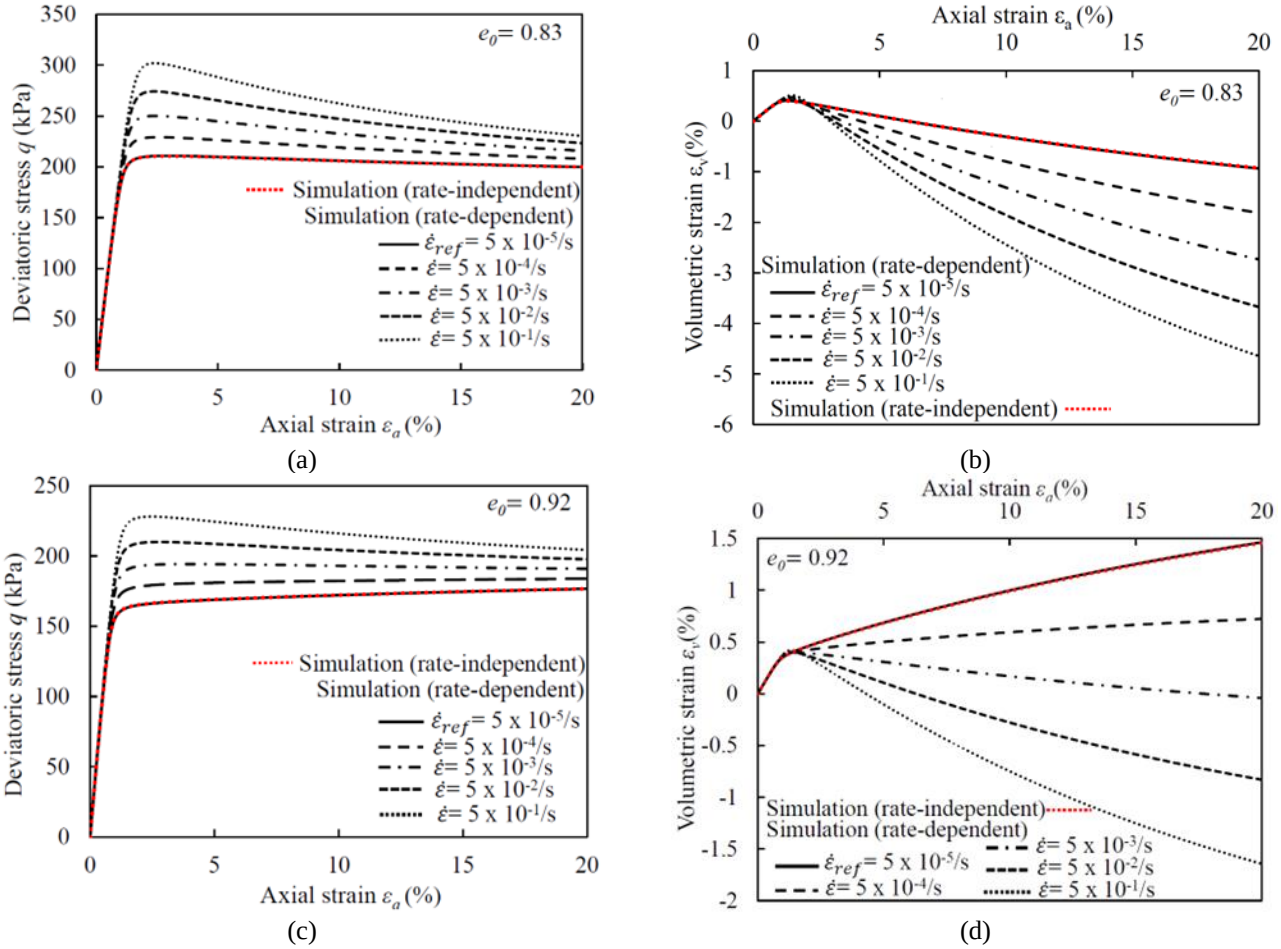

Fig. 7 Evolution of (a, c) stress-strain and (b, d) volumetric response of Toyoura sand for two different initial void ratios ($e_0 = 0.83$, 0.92, respectively) and subjected to drained triaxial condition at initial confining pressure (p_0') of 100 kPa with varying strain rate

limited to 40% and 25% in case of medium dense ($e_0 = 0.83$) and loose state ($e_0 = 0.92$), respectively. The rate of peak shear strength enhancement can be mathematically explained through a higher rate of decrease in the magnitude of state variable (Ψ) resulting in a substantial increase in the peak stress ratio (η_{ps}) for dense state in comparison to the loose one (Eq. (7)). This justification is pertinent in reference to the experimental observations reported in the literature, which confirms that the rate effects in dense sand is more pronounced due to higher tendency to dilate (Lee *et al.* 1969, Suescun-Florez and Iskander 2017). Fig. 8(b) also clearly indicates that such increase in peak strength remains nearly independent of the confinement level, except for loose sand where rate-induced strength enhancements are more pronounced at lower confinement. This might be attributed to the change in the shear deformation response of loose sands at lower confinements, i.e. from shear hardening to a shear softening one with increase in the shearing rate.

4.2 Peak friction angle

In comparison to the peak shear strength increment, the corresponding increase in the peak friction angle (Φ_p) has been found to be around 20% for dense to medium dense states and 15% for loose state as depicted in Fig. 9. Further, from Figs. 9(b) and 8(b), it can be noticed that the influence of confinement on the rate-induced enhancements of loose sand becomes quite prominent when assessed in terms of peak friction angle. It can be also inferred that a small amount of change in the friction value, due to variation in the strain rate magnitude, may impart marked difference in the estimated shear strength and hence, it is a matter of concern for in-situ soil strength tests involving intermediate to high strain rate (Watanabe and Kusakabe 2012).

4.3 Axial strain at peak shear stress

The axial strains at peak shear stress (ε_p), normalized by its corresponding value at reference strain rate ($\varepsilon_{p_{ref}}$), have been plotted in Fig. 10(a) for simulations with different initial densities and confining pressures. Simulations with higher strain rates predict an increasing trend of $\varepsilon_p/\varepsilon_{p_{ref}}$ for dense sand indicating delayed onset of peak, which becomes more prominent with increasing level of confinement. On the contrary, for medium dense and loose sands , an early onset of peak is evident with the decreasing

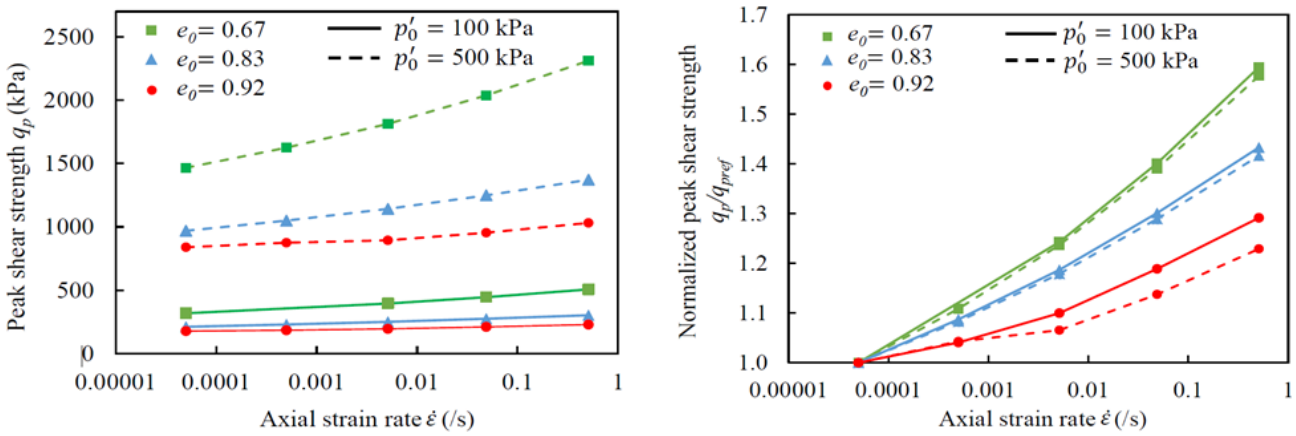

Fig. 8 Variation in the (a) peak shear strength (q_p) and (b) normalized peak shear strength ($q_p/q_{p_{ref}}$) of Toyoura sand over the selected strain rate range when subjected to drained triaxial condition at two different initial confinement (p'_0 = 100, 500 kPa) and for three initial densities (e_0 = 0.67, 0.83, 0.92)

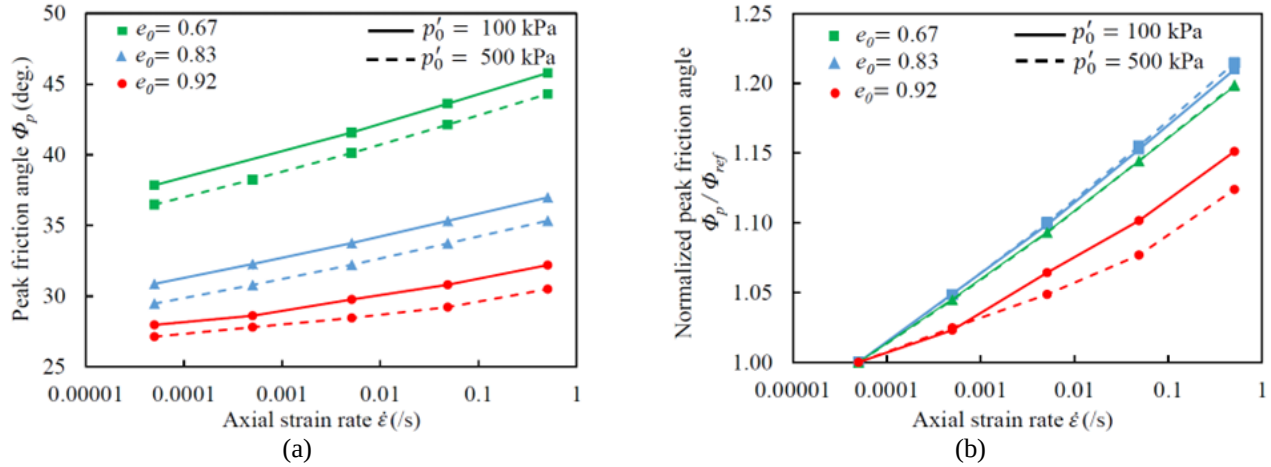

Fig. 9 Variation in the (a) peak friction angle (Φ_p) and (b) normalized friction angle ($\Phi_p/\Phi_{p_{ref}}$) of Toyoura sand over the selected strain rate range when subjected to drained triaxial condition at two different initial confinement (p'_0 = 100, 500 kPa) and for three initial densities (e_0 = 0.67, 0.83, 0.92)

trend of the $\varepsilon_p/\varepsilon_{p_{ref}}$ values. In case of loose sand, such early onset of peak becomes further significant at lesser confinement and for higher shearing rates; however, a reverse trend can be noticed for medium dense sand with respect to decrease in the confinement level. Due to the phase transformation associated with the loose sand with increasing strain rate, as illustrated in Figs. 7(c) and 7(d), the stress-strain response of the loose sand changes from a hardening to a softening one exhibiting distinct early peak. Such observation is consistent with the experimental observation reported in Yamamuro *et al.* (2011), Omidvar *et al.* (2012) and Suescun-Florez and Iskander (2017). This causes a sudden drop in the axial strain values at peak. Thus, the normalized axial strain at peak reduces suddenly due to the phase transformation in loose sand with increasing strain rate as depicted in Fig. 10(a). To investigate it further, the variation in magnitudes of ε_p have been plotted in Fig. 10(b) for medium dense and dense sand. For both the cases, the strains at peak stress have been noted to be higher for higher confinement. In case of medium dense sand at lower confinement, a gradual but continuous reduction can be noticed in the ε_p value with increasing strain rate. Whereas, at higher confinement, a sudden reduction in ε_p is evident at strain rate 5x10^{-4} /s, which then remains nearly constant with the change in strain rate. Similar to the loose state, such sudden decrease may attribute to a change of shearing behavior from hardening to a rate-induced softening type. The higher value of $\varepsilon_{p_{ref}}$ along with the reduced magnitude of ε_p for higher rates manifest the rapid reduction trend in the $\varepsilon_p/\varepsilon_{p_{ref}}$ response for the medium dense sand at higher confinement.

5. Conclusions

In the present study, the rate-dependent mechanical response of Toyoura sand has been assessed over various initial densities and confining pressure regimes. In this

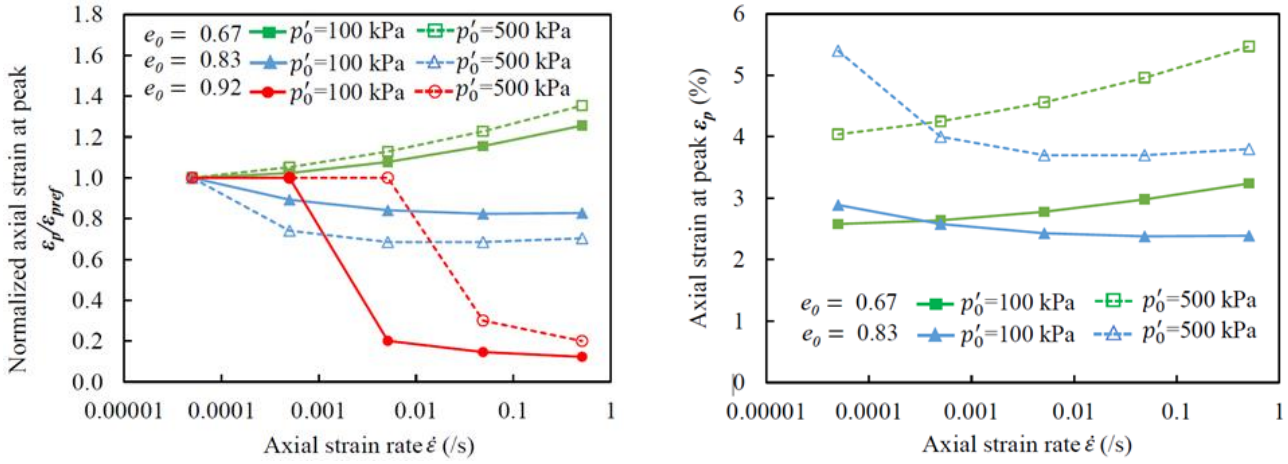

Fig. 10 Variation in (a) normalized axial strain at peak ($\varepsilon_p/\varepsilon_{p_{ref}}$) and (b) axial strain at peak (ε_p) of Toyoura sand over the selected strain rate range when subjected to drained triaxial condition at different initial confinements and void ratios

regard, a recently proposed visco-plastic model has been employed in reference to the drained triaxial experimental data on dense Toyoura sand subjected to an intermediate strain rate range of $5x10^{-5}$ /s to $5x10^{-1}$ /s. The model parameters have duly been calibrated from the test data available in the literature and the drained triaxial simulations have been carried out by writing a MATLAB code employing a fully explicit stress update algorithm. For the selected reference strain rate, the stress–strain behavior predicted from the rate-dependent simulation converge to the same as obtained from a rate-independent analysis. Further, the rate-dependent response of dense Toyoura sand, for two different initial confinements and over the reported strain rate range, can be captured with sufficient accuracy by controlling a single constitutive parameter (power law exponent *n*) in accordance with the prevailing drainage condition. In this regard, the employed model shows potential to capture some of the key features of the rate-dependent strength characteristics, which includes strength enhancement with distinct peak along with suppressed compressive response at intermediate range of strain rate.

The influence of strain rate on the peak strength, peak friction angle and strain at peak have been analyzed in detail based on the model predictions at three different density states and two initial confinements. An increase in the peak shear strength of around 60% has been observed for dense Toyoura sand over four orders of magnitude increase in the logarithmic scale of strain rate; whereas, such increase has been limited to 40% and 20% in case of medium dense and loose state, respectively. The corresponding increase in the peak friction angle has been found to be around 20-15% for a change in density state from dense to loose. However, such rate-induced strength enhancements have been observed to remain nearly independent of the level of confinement, except for loose state where such enhancement is more pronounced at lower confinements. For dense state, the strain at peak strength increases with increasing strain rate indicating a delayed peak; whereas, an early peak has been observed for medium dense to loose Toyoura sand at higher rates with decrease in the magnitude of strain at peak strength. Such variation in soil strength and stiffness characteristics further affects the design and interpretation of results for various geotechnical applications like rapid pile load testing, pile driving or jacking, dynamic compaction, installation of deep-sea anchors, design against blast loading etc., where medium to high strain rate ranges are involved. Increasing strain rate results in overestimated static bearing capacity owing to the increased shear strength from the field penetration tests. In addition, early peak followed by the pronounced post-peak softening response may influence the failure response of the geotechnical structures when subjected to loading with medium to high strain rate. Hence, it becomes imperative to consider the rate-dependent behavior of the soil along with implementation of an appropriate visco-plastic constitutive model while dealing with the geotechnical applications involving medium to high strain rate ranges.

Acknowledgments

The corresponding author would like to thank SERB (Grant No. ECR/2018/002141) for the financial support toward carrying out this research work.

References

Abrantes, A.E. and Yamamuro, J.A. (2002), "Experimental and data analysis techniques used for high strain rate tests on cohesionless soil", *Geotech. Test. J.*, **25**(2), 128-141. https://www.astm.org/gtj11356j.html.

Andrade, J.E., Chen, Q., Le, P.H., Avila, C.F. and Evans, T.M. (2012), "On the rheology of dilative granular media: bridging solid-and fluid-like behavior", *J. Mech. Phys Solids*, **60**(6), 1122-1136. https://doi.org/10.1016/j.jmps.2012.02.011.

Augustesen, A., Liingaard, M. and Lade, P. (2004), "Evaluation of time-dependent behavior of soils", *Int. J. Geomech.*, **4**(3), 137-156. https://doi.org/10.1061/(ASCE)1532-3641(2004)4:3(137).

Azeiteiro, R.J., Coelho, P.A., Taborda, D.M. and Grazina, J.C. (2017), "Critical state–based interpretation of the monotonic behavior of Hostun sand", *J. Geotech. Geoenviron. Eng.*,

143(5), 04017004. https://doi.org/10.1061/(ASCE)GT.1943-5606.0001659.

Boukpeti, N., Mroz, Z. and Drescher, A. (2004), "Modeling rate effects in undrained loading of sands", *Can. Geotech. J.*, **41**(2), 342-350. https://doi.org/10.1139/t03-077.

Casagrande, A. and Shannon, W.L. (1949), "Strength of soils under dynamic loads", *Transactions of the ASCE*, **114**(1), 755-772. https://doi.org/10.1061/TACEAT.0006198.

Chen, S.J., Yin, D.W., Jiang, N., Wang, F. and Guo, W.J. (2019), "Simulation study on effects of loading rate on uniaxial compression failure of composite rock-coal layer", *Geomech. Eng.*, **17**(4), 333-342. https://doi.org/10.12989/gae.2019.17.4.333.

Desai, C.S. and Zhang, D. (1987), "Viscoplastic models for geologic materials with generalized flow rule", *Int. J. Numer. Anal. Method. Geomech.*, **11**, 603-620. https://doi.org/10.1002/NAG.1610110606.

Doanh, T. and Ibraim, E. (2000), "Minimum undrained strength of Hostun RF sand", *Geotechnique*, **50**(4), 377-392. https://doi.org/10.1680/geot.2000.50.4.377.

Emerson, M.W. and Hendron Jr., A.J. (1971), "Measurement of stress and strain during one dimensional compression of large compacted soil and Rockfill specimens", Contract Report S-71-4. Urbana, IL: Dept. of Civil Engineering, University of Illinois.

Farr, J.V. (1986), "Loading rate effects on the one-dimensional compressibility of four partially saturated soils", Ph.D. Dissertation, University of Michigan, Michigan.

Farr, J.V. (1990), "One-dimensional loading-rate effects", *J. Geotech. Eng.*, **116**(1), 119-135. https://doi.org/10.1061/(ASCE)07339410(1990)116:1(119).

Gajo, A. and Muir Wood, D. (1999), "A kinematic hardening constitutive model for sands: the multiaxial formulation", *Int. J. Numer. Anal. Method. Geomech.*, **23**(9), 925-965. https://doi.org/10.1002/(SICI)1096-9853(19990810) 23:9<925::AID-NAG19>3.0.CO;2-M.

Hardin, B.O. and Black, W.L. (1966), "Sand stiffness under various triaxial stresses", *J. Soil Mech. Found. Eng. Div. ASCE*, **91**(2), 353-369. https://doi.org/10.1061/JSFEAQ.0000865.

Higgins, W., Chakraborty, T. and Basu, D. (2013), "A high strain-rate constitutive model for sand and its application in finite-element analysis of tunnels subjected to blast", *Int. J. Numer. Anal. Method. Geomech.*, **37**, 2590-2610. https://doi.org/10.1002/nag.2153.

Holscher, P., Van Tol, A.F. and Huy, N.Q. (2012), "Rapid pile load tests in the geotechnical centrifuge", *Soils Found.*, **52**(6), 1102-1117. https://doi.org/10.1016/j.sandf.2012.11.024.

Jackson, J.G., Ehrgott, J.Q. and Rohani, B. (1980), "Loading rate effects on compressibility of sand", *J. Geotech. Eng. Div.*, **106**(8), 839-852. https://erdclibrary.erdc.dren.mil/jspui/bitstream/11681/11052/1/MP-SL-79-24.pdf.

Karimpour, H. and Lade, P.V. (2010), "Time effects relate to crushing in sand", *J. Geotech. Geoenviron. Eng.*, **136**(9), 1209-1219. https://doi.org/10.1061/(ASCE)GT.1943-5606.0000335.

Katona, M. (1984), "Evaluation of viscoelastic cap model", *J. Geotech. Eng.*, **110**(8), 1106-1125. https://doi.org/10.1061/(ASCE)0733-9410(1984)110:8(1106).

Karunawardena, A., Oka, F. and Kimoto, S. (2011), "Elasto-viscoplastic modeling of the consolidation of Sri Lankan peaty clay", *Geomech. Eng.*, **3**(3), 233-254. https://doi.org/10.12989/gae.2011.3.3.233.

Kongkitkul, W., Tatsuoka, F., Duttine, A., Kawabe, S., Enomoto, T. and Di Benedetto, H. (2008), "Modelling and simulation of rate-dependent stress-strain behavior of granular materials in shear", *Soils Found.*, **48**(2), 175-194. https://doi.org/10.3208/sandf.48.175.

Lade, P.V. and Karimpour, H. (2010), "Static fatigue controls particle crushing and time effects in granular materials", *Soils Found.*, **50**(5), 573-583. https://doi.org/10.3208/sandf.50.573.

Lee, K.L., Seed, H.B. and Dunlop, P. (1969), "Effect of transient loading on the strength of sand", *Proceedings of the 7th International Conference on Soil Mechanics and Foundation Engineering,* Mexico.

Li, F.L., Li, J.Z. and Kongkitkul, W. (2009), "Strain rate effects on sand and its quantitative analysis", *J. Central South Univ. Technol.*, **16**(4), 658-662. https://doi.org/10.1007/s11771-009-0109-0.

Martindale, H., Higgins, W., Chakraborty, T. and Basu, D. (2010), "Two-surface viscoplastic sand model for high-rate loading", *Proceedings of International Conference on Geotechnical Engineering, Tunisia,* March.

Mokni, M. and Desrues, J. (1999), "Strain localization measurements in undrained plane-strain biaxial tests on Hostun RF sand", *Mechanics of Cohesive-frictional Materials: An International Journal on Experiments, Modelling and Computation of Materials and Structures*, **4**(4), 419-441. https://doi.org/10.1002/(SICI)10991484(199907)4:4%3C419::AID-CFM70%3E3.0.CO;2-1.

Monkul, M.M. (2013), "Influence of gradation on shear strength and volume change behavior of silty sands", *Geomech. Eng.*, **5**(5), 401-417. http://dx.doi.org/10.12989/gae.2013.5.5.401.

Mukherjee, M. (2016), "Instabilities and rate-dependency in mechanical behavior of sand", Ph.D. Dissertation, Indian Institute of Technology Kanpur, Kanpur.

Mukherjee, M., Gupta, A. and Prashant, A. (2021), "A rate-dependent model for sand to predict constitutive response and instability onset", *Acta Geotechnica*, **16**, 93-111. https://doi.org/10.1007/s11440-020-00988-8.

Omidvar, M., Iskander, M. and Bless, S. (2012), "Stress-strain behavior of sand at high strain rates", *Int. J. Impact Eng.*, **49**, 192-213. https://doi.org/10.1016/j.ijimpeng.2012.03.004.

Park, C.S. and Tatsuoka, F. (1994), "Anisotropic strength and deformation of sands in plane strain compression", *Proceedings of International conference on Soil Mechanics and Foundation Engineering,* New Delhi.

Perzyna, P. (1963), "The constitutive equations for rate sensitive plastic materials", *Q. Appl. Math.*, **20**(4), 321-332. https://doi.org/10.1090/qam/144536.

Perzyna, P. (1966), "Fundamental problems in viscoplasticity", *Adv. Appl. Mech.*, **9**, 244368. https://doi.org/10.1016/S0065-2156(08)70009-7.

Prabhu, S. and Qiu, T. (2022), "Simulation of split hopkinson pressure bar tests on sands using the discrete-element method", *Int. J. Geomech.*, **22**(2), 06021036. https://doi.org/10.1061/(ASCE)GM.1943-5622.0002262.

Safa, M., Maleka, A., Arjomand, M.A., Khorami, M. and Shariati, M. (2019), "Strain rate effects on soil-geosynthetic interaction in fine-grained soil", *Geomech. Eng.*, **19**(6), 533-542. https://doi.org/10.12989/gae.2019.19.6.533.

Safdar, M., Newson, T., Schmidt, C., Sato, K., Fujikawa, T. and Shah, F. (2021), "Shear wave velocity of fiber reinforced cemented Toyoura silty sand", *Geomech. Eng.*, **25**(3), 207-219. https://doi.org/10.12989/gae.2021.25.3.207.

Seed, H.B. and Lundgren, R. (1954), "Investigation of the effect of transient loading on the strength and deformation characteristics of saturated sands", *Am. Soc. Test. Materi.*, **54**, 1288-1306. https://www.issmge.org/uploads/publications/1/38/1969_01_0031.pdf

Shi, Z., Wood, D.M., Huang, M. and Hambleton, J.P. (2021), "Tay creep: a multi-mechanism model for rate-dependent deformation of soils", *Geotechnique*, 1-13. https://doi.org/10.1680/jgeot.21.00084.

Suescun-Florez E. and Iskander, M. (2017), "Effect of fast constant loading rates on the global behavior of sand in triaxial

compression", *Geotech. Test. J.*, **40**(1), 52-71. https://www.astm.org/gtj20150253.html.
Suescun-Florez, E., Omidvar, M., Iskander, M. and Bless, S. (2015), "Review of high strain rate testing of granular soils", *Geotech. Test. J.*, **38**(4), 511-536. https://www.astm.org/gtj20140267.html.
Tong, X. and Tuan, C.Y. (2007), "Viscoplastic cap model for soils under high strain rate loading", *J. Geotech. Geoenviron. Eng.*, **133**(2), 206-214. https://doi.org/10.1061/(ASCE)1090-0241(2007)133:2(206).
Verdugo, R. and Ishihara, K. (1996), "The steady state of sandy soils", *Soils Found.*, **36**(2), 81-91. https://doi.org/10.3208/sandf.36.2_81.
Wang, W.M., Sluys, L.J. and De Borst, R. (1997), "Viscoplasticity for instabilities due to strain softening and strain-rate softening", *Int. J. Numer. Method. Eng.*, **40**(20), 3839-3864. https://doi.org/10.1002/(SICI)10970207(19971030)40:20%3C3839::AID-NME245%3E3.0.CO;2-6.
Wang, Z. and Wong, R.C.K. (2010), "Effect of grain crushing on 1D compression and 1D creep behavior of sand at high stresses", *Geomech. Eng.*, **2**(4), 303-319. http://dx.doi.org/10.12989/gae.2010.2.4.303.
Watanabe, K. and Kusakabe, O. (2013), "Reappraisal of loading rate effects on sand behavior in view of seismic design for pile foundation", *Soils Found.*, **53**(2), 215-231. https://doi.org/10.1016/j.sandf.2013.02.003.
Whitman, R.V. and Healy, K.A. (1962), "Shearing strength of sands during rapid loading", *Transactions of ASCE*, **128**(1), 1553-1594. https://ascelibrary.org/doi/10.1061/JSFEAQ.0000411.
Whitman, R.V. (1957), "The behavior of soils under transient loading", *Proceedings of the 4th International conference on Soil Mechanics*, London.
Wood, D.M. (2004), *Geotechnical Modelling*, CRC Press (Taylor and Francis group), Boca Raton, Florida, US.
Wood, D.M. and Belkheir, K. (1994), "Strain softening and state parameter for sand modelling", *Geotechnique*, **44**(2), 335-339. https://www.icevirtuallibrary.com/doi/pdf/10.1680/geot.1994.44.2.335.
Yamamuro, J.A., Abrantes, A.E. and Lade, P.V. (2011), "Effect of strain rate on the stress-strain behavior of sand", *J. Geotech. Geoenviron. Eng.*, **137**(12), 1169-1178. https://doi.org/10.1061/(ASCE)GT.1943-5606.0000542.
Yamamuro, J.A. and Lade, P.V. (1993), "Effects of strain rate on instability of granular soils". *Geotech. Test. J.*, **16**(3), 304-313. https://www.astm.org/gtj10051j.html.

JS